Korean Journal of Remote Sensing, Vol.24, No.1, 2008, pp.65~78

A Comparative Study of Algorithms for Estimating Land Surface Temperature from MODIS Data

Myoung-Seok Suh †, So-Hee Kim, and Jeon-Ho Kang

Department of Atmospheric Science, Kongju National University, 182 Shinkwan-dong, Gongju-city 314-701, ChungCheongnam-do, Korea

Abstract : This study compares the relative accuracy and consistency of four split-window land surface temperature (LST) algorithms (Becker and Li, Kerr *et al.*, Price, Ulivieri *et al.*) using 24 sets of Terra (Aqua)/Moderate Resolution Imaging Spectroradiometer (MODIS) data, observed ground grass temperature and air temperature over South Korea. The effective spectral emissivities of two thermal infrared bands have been retrieved by vegetation coverage method using the normalized difference vegetation index. The intercomparison results among the four LST algorithms show that the three algorithms (Becker-Li, Price, and Ulivieri *et al.*) show very similar performances. The LST estimated by the Becker and Li's algorithm is the highest, whereas that by the Kerr *et al.*'s algorithm is the lowest without regard to the geographic locations and seasons. The performance of four LST algorithms is significantly better during cold season (night) than warm season (day). And the LST derived from Terra/MODIS is closer to the observed LST than that of Aqua/MODIS. In general, the performances of Becker-Li and Ulivieri *et al* algorithms are systematically better than the others without regard to the day/night, seasons, and satellites. And the root mean square error and bias of Ulivieri *et al.* algorithm are consistently less than that of Becker-Li for the four seasons.

Key Words : Land surface temperature, split-window algorithm, MODIS.

1. Introduction

The land surface temperature (LST) plays an important role in the physics of land surface through controling the processes of energy and water exchange between the land surface and the atmosphere. So, the LST is a useful element for the wide range of applications, agriculture, numerical and climate modeling community. However, operational observation of LST is far from the needs of application community both in spatial and temporal scale. Because the LST is a highly variable in space and time, and too difficult to observe. Therefore, retrieval of LST from satellite data can be regarded as an effective means for the operational observation of LST. Compared to the ground observed LST, the LST retrieved from meteorological satellite data can be defined as a weighted average temperature of

Received 14 February 2008; Accepted 20 February 2008.

† Corresponding Author: Myoung-Seok Suh (sms416@kongju.ac.kr)

various components which constitute a pixel.

For the first time, Price (1984) retrieved the LST from satellite data using split-window method. Theoretical possibility for the retrieval of LST from satellite data using split-window method was shown by Becker and Li (1990). In general, the coefficients of LST retrieval equations have been obtained from linear regression between satellite data and simulated data using radiative transfer model for wide ranges of surface and atmospheric conditions, and viewing geometry. Various types of algorithms have been developed for the retrieval of LST from meteorological satellite data during the last 20 years (e.g., Kerr *et al.*, 1992; Watson, 1992; Ulivieri *et al.*, 1994; Wan and Dozier, 1996; Coll *et al.*, 2005; Wan *et al.*, 2005). Among the various types of algorithms, split-window type is most commonly used because it is not only simple but also accurate in the estimation of LST. It is based on the two assumptions: One is that the atmospheric effect can be minimized by using the differential absorption in two adjacent window channels in the 10.0 ~ 12.5 μm, and the other is that the emissivity of thermal channels over land surface are avaliable.

Recently, the various background data (e.g., land cover and vegetation index) and methods for the estimation of spectral emissivity have been developed (Salisbury and D'Aria, 1992; Valor and Caselles, 1996; Peres and DaCamara, 2002). And the quality of satellite data has been significantly improved in radiometric resolution (8bits --> 10bits), navigation, channels (e.g., Moderate Resolution Imaging Spectroradiometer (MODIS) with 36 channels) and signal to noise ratio. Also, the LST retrieval algorithms are clearly improved through inclusion of satellite viewing angle, surface emissivity, total precipitable water vapor and the atmospheric lower boundary layer temperature (Wan and Dozier, 1996; Sobrino and Romaguera, 2004; Wan *et al.*, 2005). As the results, the quality of retrieved LST is being improved steadily.

In spite of the enormous efforts for the improvement of LST algorithms from satellite data, the retrieved LST is not readily available due to the poor quality. The insufficient quality of retrieved LST is mainly caused by the combined effects of spectrally and temporally varying emissivity according to the surface types, and the absorption and emission of atmospheric water vapor (Becker and Li, 1990). Also the insufficiency of ground measured LST for the validation of retrieved LST and the undetermined procedures for scaling-up from "point" measurements to the pixel values are another interfering factors (Coll *et al.*, 2005).

Various validation efforts appear to be reaching the consensus that root-mean-squared (rms) accuracies of 1~3°C are possible (Prata and Cechet, 1999; Han *et al.*, 2004; Coll *et al.*, 2005). Accuracies of 3°C are of marginal use, while accuracies of 1°C are potentially of great benefit in many applications (Prata and Cechet, 1999). In addition to that, the accuracies of LST algorithms are clearly dependent on the atmospheric conditions and surface properties. In other words, the performances of LST algorithms are highly variable according to the regional environments, such as climatic characteristics and geographic locations. So, comparative studies about the different LST algorithms have been performed by many authors (Vazquez *et al.*, 1997; Han *et al.*, 2004). They emphasized the necessity of choosing or developing the optimized LST retrieval algorithm for the given regional environments. Therefore comparative study on the accuracies of various LST algorithms over the South Korea has a meaning for choosing or developing the optimized LST algorithm. It is more meaningful because development of LST algorithms from meteorological satellite data are not systematically performed in this region except for the

few studies (Choi *et al.*, 1986; Shin *et al.*, 2004).

The purpose of this study is to investigate the relative accuracies of various LST algorithms using MODIS and ground measured air temperature over the South Korea. And sensitivity of LST algorithms to the control parameters, such as the LST, fraction of vegetation and spectral emissivity are analysed. This results can be used as background informations in the development of LST retrieval algorithm for the forthcoming Communication, Ocean and Meteorological Satellite (COMS) data.

2. Data and Methods

1) Data

The radiances of thermal infrared channels measured by the satellite radiometers are mainly affected by the atmospheric conditions (e.g., cloud, temperature and water vapor profile, aerosol), and surface conditions (temperature and emissivity), which are varying with time and space. As a result, unknown parameters are always greater than the equations when split-window methods are used for the LST retrieval, through combinations of two or three thermal infrared channels. To overcome this unresolved problem, most of the split-window methods have been developed on the assumption that the effective spectral emissivities are known.

In this study, we used the land cover map, normalized difference vegetation index (NDVI) and emissivity look up table made by Peres and DaCamara (2002) to calculate the effective spectral emissivity of thermal infrared channels. To compare the performance of LST algorithms according to the various season and time, 24 cases data in two thermal infrared bands (IR 31: 10.8μm, IR 32: 12.0μm) over the Korean Peninsula measured by MODIS/Terra and Aqua were used (Table 1). We selected 24 satellite data which have minimum cloudy pixels for day and night by visual inspection. And hourly air temperature and 1 minute grass temperature observed at the 70 ground stations and 5 agriculture stations by Korean Meteorological Administration were used as the reference data to evaluate the relative accuracy of LST algorithms.

The land cover map over the Korean Peninsula used in this study was classified by Kang *et al.* (2005) using the time series of NDVI derived from two years (2003~2004) MODIS data. The definition of land covers follows the International Geosphere-Biosphere Program (IGBP)'s criteria to use the emissivity look up table (Peres and DaCamara, 2002). The monthly NDVI data obtained from the 2 years (2003-2004) Aqua/MODIS 1km data by maximum value composite method were also used for the calculation

Table 1. Summary of Aqua and Terra MODIS images used in this study

	Satellite	Year	Date	LST
I	Aqua/MODIS (day)	2004	4 Jan.	13:41
		2004	17 Feb.	14:06
		2004	26 Mar.	13:29
		2004	9 Apr.	13:41
		2004	23 Jul.	13:36
		2004	12 Aug.	13:12
		2004	30 Oct.	14:07
		2004	6 Nov.	14:13
II	Terra/MODIS (day)	2004	21 Oct.	10:58
		2004	7 Nov.	11:40
		2004	15 Nov.	10:51
		2005	21 Jan.	11:22
	Aqua/MODIS (day)	2004	21 Oct.	14:13
		2004	7 Nov.	13:17
		2004	15 Nov.	14:06
		2005	21 Jan.	12:59
III	Terra/MODIS (night)	2004	27 Oct.	23:02
		2004	30 Oct.	21:55
		2004	7 Nov.	22:43
		2005	21 Jan.	22:25
	Aqua/MODIS (night)	2004	18 Feb.	02:08
		2004	31 Oct.	02:08
		2004	7 Nov.	02:14
		2005	21 Feb.	02:50

of temporal variation of spectral emissivity.

2) Methods

(1) Retrieval of Effective Emissivity

Temporal variation of effective spectral emissivity of land surface was calculated using Valor and Caselles (1996)'s vegetation coverage method (VCM), by the linear combination of the fraction of vegetation and ground for the given land cover.

$$\varepsilon_i = \varepsilon_{i,v} \times FVC + \varepsilon_{i,g} \times (1 - FVC) \quad (1)$$

where ε_i is the effective surface spectral emissivity of each channel (IR 31, IR 32), $\varepsilon_{i,v}$ and $\varepsilon_{i,g}$ are the maximum emissivity of the vegetation (v) and the ground (g) for the given land cover types (i), respectively. We used the look-up table of emissivity generated by Peres and DaCamara (2002). FVC is a fraction of vegetation coverage (FVC) and calculated using Kerr *et al.* (1992)'s method.

$$FVC = \frac{NDVI - NDVI_{CS}}{NDVI_{CV} - NDVI_{CS}} \quad (2)$$

where, the $NDVI_{CV}$ and $NDVI_{CS}$ indicate the NDVI values when the pixel is fully occupied by vegetation (completely vegetated) or ground (completely soil), respectively. The values of $NDVI_{CV}$ and $NDVI_{CS}$ are decided like the other studies (Gutman and Ignatov, 1998; Sobrino and Raissouni, 2000) as 0.8 and 0.13, respectively.

(2) Retrieval of LST

Numerous LST retrieval algorithms have been developed and evaluated using polar orbit and/or geostationary meteorological satellite, such as NOAA/AVHRR (Advanced Very High Resolution Radiometer), Terra/MODIS, and EUMETSAT/ SEVIRI (Spinning Enhanced Visible and Infrared Imager). Various combinations of thermal infrared channels from two-channel to four-channel have been developed and evaluated (e. g., Price, 1984; Becker and Li, 1990; Kerr *et al.*, 1992; Wan and Dozier, 1996; Sikorski and Kealy, 2002; Sobrino and Romaguera, 2004). Many works showed that the best combination is IR10.8 and IR12.0 μm because the two bands are more transparent, and they are carried at almost all the meteorological satellites (e.g., Sobrino and Romaguera, 2004). In addition, their effective emissivities are not only close to unity but also less variable than other thermal channels. To investigate the current status and relative accuracy of different LST algorithms, we selected 4 sets of two-channel LST algorithm among the numerous algorithms. The selected LST algorithms are as follows:

① Price (1984)

$$T_s = [T_{31} + 3.33(T_{31} - T_{32})]\left(\frac{5.5 - \varepsilon_{31}}{4.5}\right) + 0.75 T_{32}(\varepsilon_{31} - \varepsilon_{32}) \quad (3)$$

② Becker and Li (1990)

$$T_s = 1.274 + \left(1 + 0.15616\frac{1-\varepsilon}{\varepsilon} - 0.482\frac{\Delta\varepsilon}{\varepsilon^2}\right)\frac{T_{31} + T_{32}}{2} + \left(6.26 + 3.98\frac{1-\varepsilon}{\varepsilon} + 38.33\frac{\Delta\varepsilon}{\varepsilon^2}\right)\frac{T_{31} - T_{32}}{2} \quad (4)$$

$$\varepsilon = \frac{(\varepsilon_{31} + \varepsilon_{32})}{2}, \Delta\varepsilon = \varepsilon_{31} - \varepsilon_{32} \quad (4\text{-}1)$$

③ Kerr *et al.* (1992)

$$T_s = f_v T_{veg} + (1 - f_v) T_{soil} \quad (5)$$

$$T_{veg} = T_{31} + 2.6(T_{31} - T_{32}) - 2.4 \quad (5\text{-}1)$$

$$T_{soil} = T_{31} + 2.1(T_{31} - T_{32}) - 3.1 \quad (5\text{-}2)$$

④ Ulivieri *et al.* (1994)

$$T_s = T_{31} + 1.8(T_{31} - T_{32}) + 48(1 - \varepsilon) - 75\Delta\varepsilon \quad (6)$$

where T_{31}, T_{32} and ε_{31}, ε_{32} are brightness temperature and emissivity of MODIS channels 31 and 32, respectively. f_v is a fraction of vegetation for the given pixel. T_{soil} and T_{veg} are soil temperature and vegetation temperature, respectively.

The process for the LST retrieval from MODIS

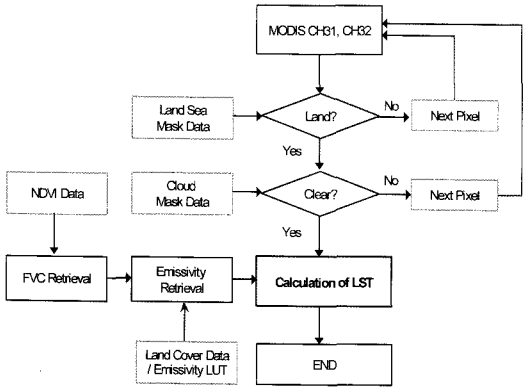

Fig. 1. Block diagram of the LST retrieval processes.

channels 31 and 32 is shown in Fig. 1. LST can be retrieved only for the clear pixel, so it is necessary to eliminate the cloud-contaminated pixels before the LST retrieval. To minimize the cloud contamination problems, we selected the relatively clear data through a visual inspection of visible channel image. And a simple threshold technique is applied to eliminate the cloud contaminated pixels because this study does not focus on the accuracy of cloud detection algorithm. The most difficult problem in the threshold technique is to determine the threshold values (e.g., Saunders and Kriebel, 1988, Suh and Lee, 1999). In this study, we used the threshold values dynamically for case by case because the properties (especially for LST and cloud top temperature) of land and cloud are highly variable according to the geographic locations and seasons.

3. Results

Fig. 2 shows the effective emissivity of MODIS channels 31 and 32 derived from monthly NDVI and land cover map using VCM for March and August. The emissivity maps show a spatial, temporal, and spectral variations, generally greater at the vegetated area and channel 32 than the urban area and channel 31. It shows that the variations of effective spectral emissivity are closely linked with land cover type and vegetation phenology. So, the emissivities over the urban and evergreen area show a relatively weak temporal variation, whereas, those over crop and deciduous type area show a strong temporal variation.

The sensitivities of spectral effective emissivity to the errors of $\pm 10\%$ and $\pm 20\%$ in the FVC are shown in Table 2. As shown in other studies, the impacts of FVC errors on the spectral emissivity are almost negligible in all the land cover types (e.g., Vázquez *et al.*, 1997). It indicates that the VCM is a relatively stable method in the calculation of FVC.

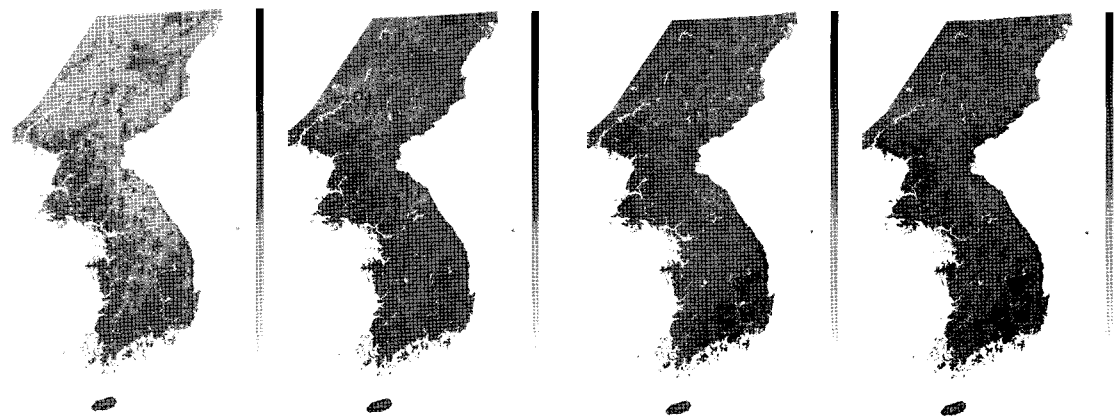

(a) (b)

Fig. 2. Effective emissivity map of (a) March and (b) August for MODIS Ch 31(left) and Ch 32(right) derived from monthly NDVI and land cover map using VCM.

Table 2. Sensitivities of the effective spectral emissivity (ESE) to the errors in FVC. ΔEm31 and ΔEm32 represent the differences of ESE of MODIS channel 31 and 32 when FVC has -10%(-20%) errors and FVC has +10%(+20%) errors

IGBP Land Cover	FVC ±10%		FVC ±20%	
	ΔEm31	ΔEm32	ΔEm31	ΔEm32
1 - Evergreen Needleleaf Forest	0.0002	0.0002	0.0004	0.0004
2 - Evergreen Broadleaf Forest	0.0002	0.0002	0.0004	0.0004
3 - Deciduous Needleleaf Forest	0	0	0.0001	0
4 - Deciduous Broadleaf Forest	0	0	0.0001	0
5 - Mixed Forest	0.0001	0.0001	0.0002	0.0002
6 - Closed Shrublands	0.0001	0.0001	0.0003	0.0002
7 - Open Shrublands	0.0001	0.0001	0.0003	0.002
8 - Woody Savannas	0	0	0.0001	0
9 - Savannas	0	0	0	0
10 - Grasslands	0	0	0	0
11 - Permanent Wetlands	0	0	0	0
12 - Croplands	0.0001	0.0001	0.0002	0.0002
13 - Urban and Built up	0.0002	0	0.0003	0.0001
14 - Cropland/Natural Vegetation	0	0	0.0001	0
15 - Snow and Ice	0	0	0	0
16 - Barren or Sparsely Vegetated	0.0001	0	0.0002	0.0001
17 - Water	0	0	0	0

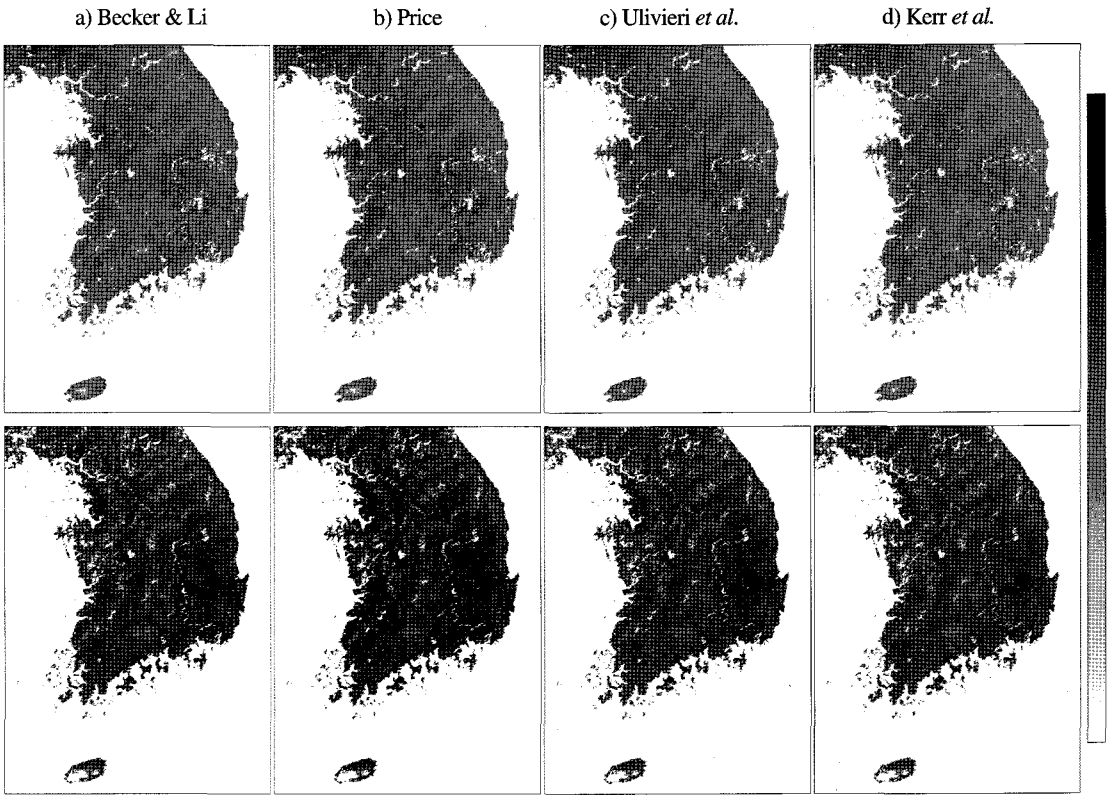

Fig. 3. Sample Images of LST derived from four different split window algorithms. Black indicates a warmer LST(scale bar: 260~330K) and white indicates rivers, dams and other water reservoirs. Upper and lower images are LST of 26 March, 2004 and 12 August, 2004, respectively.

Spatial distribution of LST over South Korea retrieved by four algorithms are shown in Fig. 3. White color (Southern part of Jeju island, Seoul area and northern part) means the pixels contaminated by cloud. The white lines and small areas over Choongchung and Gangwon area mean the rivers and dams. Spatial variations of LST are closely linked with the land cover and topography of the Korean Peninsula. The LST is clearly warmer at the major cities, such as Daegu, Gwangju, and Daejeon than suburban and mountain areas due to the urban heat island effects. As the results, LST is the highest and lowest at the urban area and high mountain area, respectively. Although the spatial patterns of LST are very similar among the four LST algorithms, the LST values are slightly different among the algorithms. Becker and Li's algorithm produces the highest LST, whereas Kerr *et al.*'s algorithm produces the lowest LST without regard to the geographic locations (land cover and topography) and seasons.

The LST retrieved by four algorithms are different systematically regardless of the values of LST (Fig. 4), although the differences and order among the four algorithms vary with seasons. The LST calculated by Becker and Li is the highest and that by Kerr *et al.* is the lowest regardless of the season and LST values. Whereas, the differences between Ulivieri *et al.* and Price are strongly dependent on the season and LST values. So, the LST by Ulivieri *et al.* is warmer than that by Price during cold season (winter), but the order is reversed during the warm season (Spring, Summer, and Fall) and the differences are

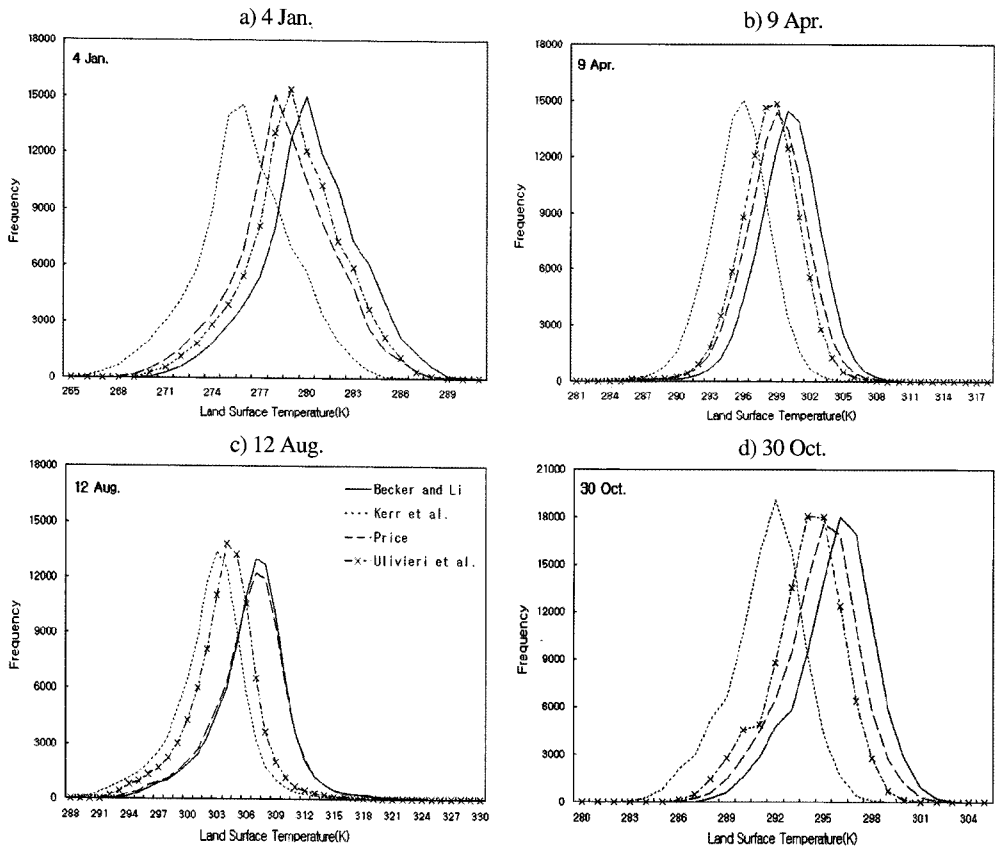

Fig. 4. Histogram of LST retrieved by the four LST algorithms for 4 selected days. Solid, dotted, dashed and dashed with 'x' represent the LST by Becker and Li, Kerr *et al.*, Price and Ulivieri *et al.*, respectively.

proportional to the LST. The reverse in the LST values derived by Price and Ulivieri *et al.* with season are related to the LST equations (See the eqs. (3) and (6)). The Price algorithm is more sensitive to the brightness temperature difference (ΔT) and emissivity of channel 31(ε_{31}) than the that by Ulivieri *et al.* So, the increases of ΔT and ε_{31} during summer resulted in the more increase of the Price's LST than Ulivieri *et al.*'s one.

To investigate the differences and similarities among the LST algorithms, comparison on the 6 pairs of algorithms were performed (Fig. 5). The correlations between selected two LST algorithms are very high without regard to the pair, ranging from 0.992 to 0.999. The two pairs (Kerr *et al.*-Becker & Li, Kerr *et al.*-Ulivieri *et al.*) show the maximum correlations. Whereas the RMSE varies significantly from 0.67 to 4.52 according to the pair. The RMSEs of the pairs coupled with Kerr *et al.* are considerably greater than those of other pairs. And the magnitude

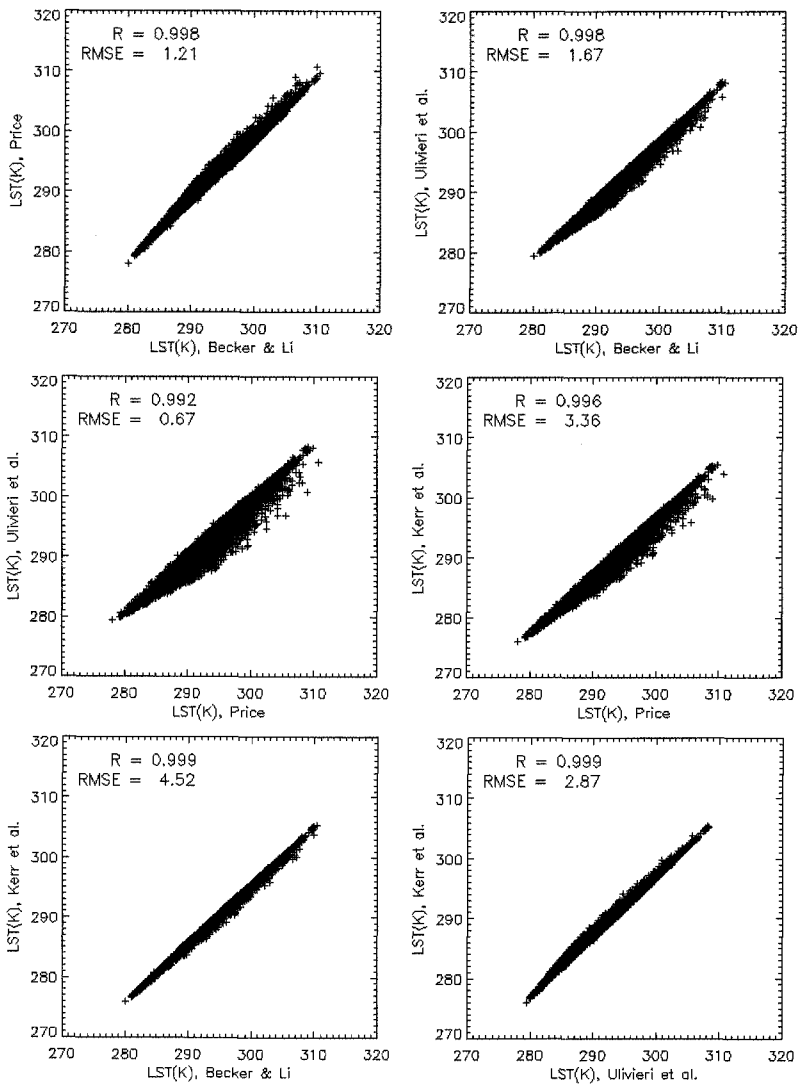

Fig. 5. Comparison of LST retrieved by the paired split window algorithms for 6 March, 2004.

of spread also varies according to the pair, with the widest spread at the Ulivieri *et al.*-Price and Kerr *et al.*-Price pairs. In general, Kerr *et al.* is systematically underestimate the LST compared to the others. Comparing with other results, such as Han *et al.* (2004) and Vazquez *et al.* (1997), correlations are very similar without regard to the pairs but the RMSEs are different according to the pairs.

Comparison results between paired LST algorithms for the 8 selected cases are shown in Table 3. The correlations among the paired algorithms are very high and statistically indistinguishable, but the average RMSE and bias of the pairs are strongly dependent on the combination method, ranging from 1.16 (-0.76) to 4.33 (4.32). In general, the RMSE and biases of the pairs are less than 1.84 K except for the pairs coupled with Kerr *et al.* The best and worst fitted pairs are Becker-Price and Becker-Kerr *et al.*, respectively. The similar values of RMSE and biases among pairs for the 8 selected cases indicate that the differences between algorithms are very systematic. However, the sign and magnitude of biases at the Ulivieri *et al.* -Price pair are changed according to the season, with positive and small during cold season, negative and large during warm season. The reasons for changes of sign and magnitude are explained in Fig. 4.

As far as we know, the ground observed LST data over South Korea with good quality are not usable for the validation of LST derived from satellite. So we used the air temperature data observed by AWS as a surrogate. Before the comparison between AWS and MODIS LST data, collocation of two data is performed, because the representatives of AWS and

Table 3. Comparison results between paired split-window algorithms for the LST from Aqua/MODIS data

Pairs	Date	R	RMSE (K)	Bias (K)	Pairs	Date	R	RMSE (K)	Bias (K)
Becker - Price	4 Jan.	0.998	1.66	1.65	Ulivieri - Kerr	4 Jan.	0.999	3.26	3.25
	17 Feb.	0.998	1.79	1.77		17 Feb.	0.999	3.17	3.17
	26 Mar.	0.998	1.21	1.18		26 Mar.	0.999	2.87	2.87
	9 Apr.	0.998	1.19	1.17		9 Apr.	0.999	2.73	2.73
	23 Jul.	0.991	0.59	0.11		23 Jul.	0.996	1.39	1.34
	12 Aug.	0.997	0.38	0.17		12 Aug.	0.998	1.38	1.35
	30 Oct.	0.995	1.02	0.99		30 Oct.	0.996	2.45	2.44
	6 Nov.	0.995	1.46	1.43		6 Nov.	0.997	2.88	2.87
	Ave.	0.996	1.16	1.06		Ave.	0.998	2.52	2.50
Becker - Ulivieri	4 Jan.	0.999	1.10	1.09	Ulivieri - Price	4 Jan.	0.996	0.63	0.56
	17 Feb.	0.998	0.96	0.93		17 Feb.	0.992	0.96	0.84
	26 Mar.	0.998	1.67	1.65		26 Mar.	0.992	0.67	-0.47
	9 Apr.	0.999	1.73	1.72		9 Apr.	0.996	0.63	-0.55
	23 Jul.	0.996	3.03	2.99		23 Jul.	0.981	3.04	-2.89
	12 Aug.	0.996	2.90	2.87		12 Aug.	0.989	2.80	-2.71
	30 Oct.	0.996	1.90	1.89		30 Oct.	0.986	0.98	-0.90
	6 Nov.	0.996	1.43	1.41		6 Nov.	0.985	0.49	0.03
	Ave.	0.997	1.84	1.82		Ave.	0.995	1.27	-0.76
Becker- Kerr	4 Jan.	1.000	4.26	4.25	Price - Kerr	4 Jan.	0.998	2.62	2.61
	17 Feb.	0.999	4.18	4.18		17 Feb.	0.996	2.44	2.41
	26 Mar.	0.999	4.52	4.52		26 Mar.	0.996	3.36	3.30
	9 Apr.	0.999	4.45	4.45		9 Apr.	0.997	3.29	3.28
	23 Jul.	0.997	4.34	4.33		23 Jul.	0.988	4.29	4.23
	12 Aug.	0.998	4.24	4.23		12 Aug.	0.994	4.09	4.06
	30 Oct.	0.998	4.34	4.33		30 Oct.	0.996	3.35	3.34
	6 Nov.	0.999	4.28	4.28		6 Nov.	0.994	2.86	2.85
	Ave.	0.998	4.33	4.32		Ave.	0.996	3.29	3.26

MODIS are different in spatial resolution. To minimize the differences of spatial representatives and observation time between two data, we used the 3 ×3 MODIS pixels and the pixels with the temporal difference less than 5 minutes.

Comparison results with observed air temperature by AWS and estimated LST by four different algorithms for the 8-selected cases are shown in Table 4. In general, the performance of all the LST algorithms is significantly better during cold season than warm season. And the differences among algorithms are smaller than that of any single algorithm among seasons. The LST derived by four LST algorithms are greater than the air temperature of AWS for all seasons, especially during spring and summer. This overestimation is quite reasonable because the LST is higher than air temperature during day time, especially for the afternoon time (Fig. 6) of the warm season.

Fig. 6 shows the diurnal variations of LST and air temperature at Andong and Cheolwon agricultural stations for clear days during winter and summer. The diurnal variations of LST and air temperature clearly depend on the seasons and geographic locations. The difference between LST and air temperature is relatively small during night time whereas that is very large during day time, especially during summer. It suggests that the air temperature during night time and cold season can be used as a reference temperature for the validation of LST. Whereas, the air temperature during day time, especially warm season, can't be used as a reference temperature for the validation of LST.

Comparison results with the observed LST (observed in agriculture weather stations) and the estimated LST by the four different algorithms for the day/night conditions and two satellites are shown in Table 5. The performances of four LST algorithms are systematically higher during night time than during day time. And the LSTs derived by the four algorithms using Terra/MODIS are more accurate than those by Aqua/MODIS, although the differences in correlations between two satellites are not significant. In general, the performances of the

Table 4. Comparison results with observed air temperature by AWS and estimated LST by four algorithms for the selected 8 cases

		R	R^2	RMSE(K)	Bias(K)
4 Jan. (13:41 LST)	Becker and Li	0.808	0.653	2.38	-1.44
	Ulivieri *et al.*	0.805	0.648	1.83	-0.29
	Price	0.806	0.650	1.95	0.24
	Kerr *et al.*	0.807	0.651	3.44	2.89
	Average	0.81	0.65	2.40	0.35
17 Feb. (14:06 LST)	Becker and Li	0.681	0.656	2.53	-0.23
	Ulivieri *et al.*	0.642	0.464	2.75	0.81
	Price	0.705	0.412	2.89	1.54
	Kerr *et al.*	0.666	0.497	4.79	4.06
	Average	0.67	0.51	3.24	1.54
26 Mar. (13:29 LST)	Becker and Li	0.494	0.444	10.05	-9.77
	Ulivieri *et al.*	0.490	0.449	8.43	-8.11
	Price	0.494	0.244	8.83	-8.49
	Kerr *et al.*	0.503	0.240	5.63	-5.16
	Average	0.50	0.34	8.23	-7.88
9 Apr. (13:41 LST)	Becker and Li	0.343	0.244	8.37	-7.63
	Ulivieri *et al.*	0.340	0.253	6.79	-5.90
	Price	0.344	0.396	7.25	-6.33
	Kerr *et al.*	0.341	0.392	4.56	-3.04
	Average	0.34	0.32	6.74	-5.72
23 Jul. (13:36 LST)	Becker and Li	0.234	0.479	7.22	-5.30
	Ulivieri *et al.*	0.245	0.496	4.80	-2.03
	Price	0.230	0.053	7.57	-5.34
	Kerr *et al.*	0.254	0.065	4.58	-0.53
	Average	0.24	0.27	6.04	-3.30
12 Aug. (13:12 LST)	Becker and Li	0.374	0.140	5.69	-3.76
	Ulivieri *et al.*	0.354	0.125	4.15	-0.55
	Price	0.390	0.152	5.77	-3.78
	Kerr *et al.*	0.370	0.137	4.17	0.84
	Average	0.37	0.14	4.95	-1.81
30 Oct. (14:07 LST)	Becker and Li	0.630	0.058	2.33	-1.21
	Ulivieri *et al.*	0.629	0.396	2.10	0.78
	Price	0.615	0.378	2.06	-0.15
	Kerr *et al.*	0.626	0.392	3.83	3.29
	Average	0.63	0.31	2.58	0.68
6 Nov. (14:13 LST)	Becker and Li	0.700	0.490	3.06	-2.06
	Ulivieri *et al.*	0.692	0.479	2.32	-0.54
	Price	0.699	0.397	2.36	-0.58
	Kerr *et al.*	0.704	0.396	3.25	2.36
	Average	0.70	0.44	2.75	-0.20

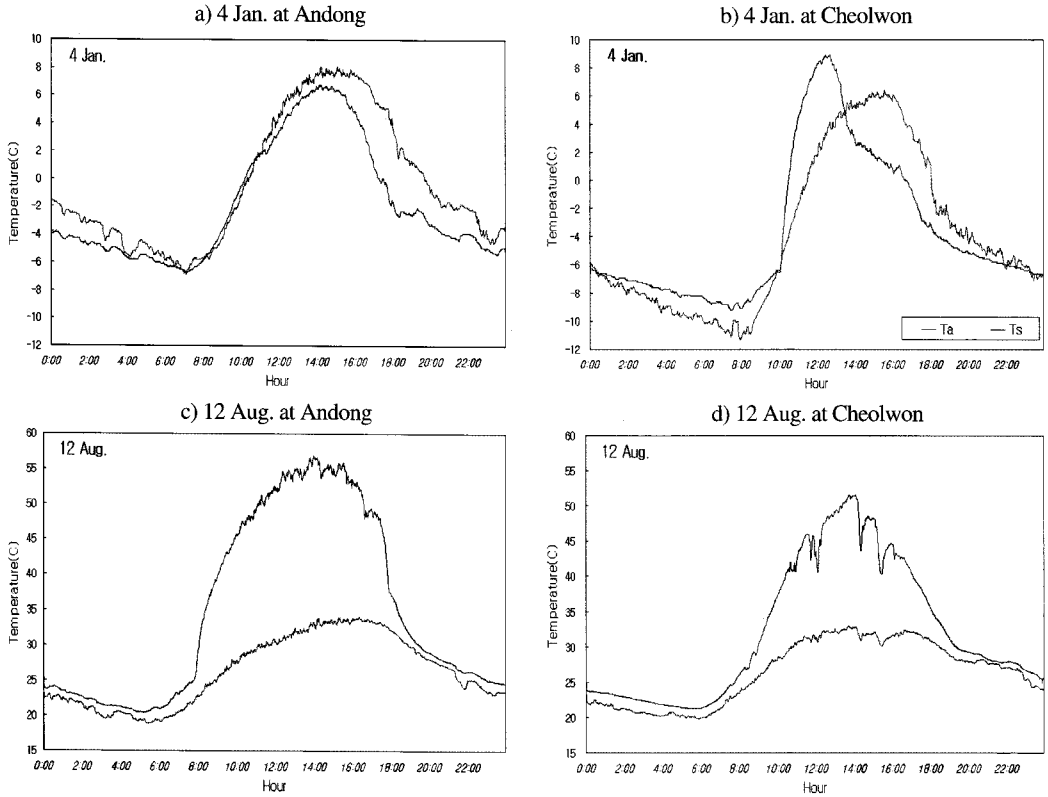

Fig. 6. Comparison of diurnal variation of land surface temperature and air temperature observed at the two agriculture weather stations for clear days. Black and grey lines mean the LST and air temperature, respectively.

Table 5. Summary of comparison results with observed LST (observed in agriculture weather station) and estimated LST by four algorithms for the day/night conditions and two satellites

	Algorithms	Terra/MODIS			Aqua/MODIS		
		R	RMSE(K)	Bias(K)	R	RMSE(K)	Bias(K)
Day	Becker/Li	0.910	3.8	-1.2	0.917	4.0	1.6
	Ulivieri *et al.*	0.908	3.7	0.5	0.912	5.0	3.4
	Price	0.906	4.9	3.2	0.927	6.8	5.8
	Kerr *et al.*	0.909	6.1	4.9	0.919	8.5	7.7
	Day Ave.	0.91	4.63	1.85	0.92	6.08	4.63
Night	Becker/Li	0.965	2.2	-1.1	0.963	2.5	1.3
	Ulivieri *et al.*	0.965	1.8	0.2	0.963	3.1	2.3
	Price	0.967	3.7	3.3	0.967	6.4	6.1
	Kerr *et al.*	0.967	5.0	4.7	0.965	7.4	7.1
	Night Ave.	0.97	3.17	1.77	0.96	4.85	4.20

algorithms by Becker and Li, and Ulivieri *et al.* are clearly better than the others without regard to the day/night and satellites.

Fig. 7 shows the sensitivity of LST algorithms due to the $\pm 1\%$ error in emissivity as a function of T_{31}. The Kerr *et al.*'s algorithm is not shown in this figure because it does not have emisisvity term explicitly. The deviation shown in Fig. 7 can be regarded as a maximum value for the given temperature and emissivity error because the maximum deviation is

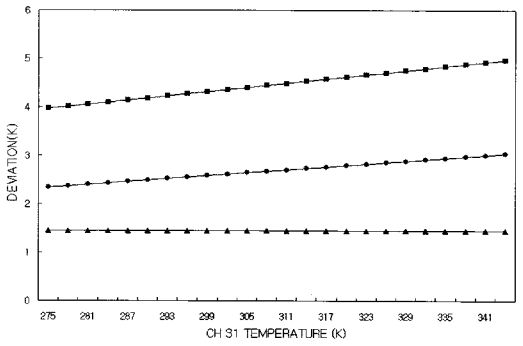

Fig. 7. Error propagation in LST due to $\pm 1\%$ error in emissivity as a function of T_{31}. Assuming $T_{31} - T_{32} = 1K$. Surface emissivity fixed to $\varepsilon_{31} = 0.96$, $\varepsilon_{32} = 0.97$. Filled box, circle and triangle mean the Price, Becker and Li, and Ulivieri *et al.*, respectively.

selected among the various combination of emissivity errors in the channels 31 and 32. The sensitivity of LST algorithm to the emissivity error is the greatest in the Price. Whereas, the Ulivieri *et al.* algorithm is the least sensitive to the emissivity error and surface temperature changes.

4. Summary and Discussion

Land surface temperature (LST) is required for a variety of climatic, hydrologic, ecological, and biogeochemical studies. Many types of algorithms were developed for the retrieval of LST using satellite data. Split-window algorithms were widely used because of computational efficiency, ease of application and accuracy. In this study, comparison of four different split-window algorithms (Becker and Li, Kerr *et al.*, Price, Ulivieri *et al.*) has been discussed using MODIS/Terr (Aqua), and ground observed LST and air temperature over South Korea. As far as we know, there is no observed LST data in South Korea suitable for the validation of LST derived from MODIS data. So we used the air temperature and grass temperature for the validation of LST.

The effective spectral emissivities of thermal infrared channels (MODIS channels 31 and 32) were retrieved by vegetation coverage method (Kerr *et al.*, 1992) using the fraction of vegetation cover (FVC) derived from normalized difference vegetation index. FVC and emissivity over the Korean Peninsula varied from 0.05 (0.96) to 0.8 (0.99) according to the season and land cover. The sensitivity analysis of emissivity to the land cover and FVC error showed that emissivity is more influenced by land cover error than by FVC error.

The intercomparison results among the four LST algorithms showed that the Becker-Li and Price, Ulivieri *et al.*, and Price algorithms are statistically very similar, whereas Becker-Li and Kerr *et al.*, Price and Kerr *et al.* algorithms are statistically quite different. In general, Becker and Li's algorithm produces the highest LST, whereas Kerr *et al.*'s algorithm produces the lowest LST without regard to the geographic locations (land cover and topography) and seasons.

In general, the performance of four LST algorithms is significantly better during cold season than warm season. And the differences among algorithms are smaller than that of an any single algorithm among seasons. The four LST algorithms overestimated the LST compared to the air temperature of AWS for all season, especially during spring and summer. This overestimation is reasonable because the LST is higher than the air temperature during day time, especially for the afternoon time of warm season.

The performance of four LST algorithms are systematically superior during night time than during day time. And the LST derived from Terra/MODIS is closer to the observed LST than that of Aqua/MODIS. In general, the performances of Becker-Li and Ulivieri *et al.* algorithms are clearly better than the others without regard to the day/night, season and satellites. And the RMSE and bias of Ulivieri *et al.*

algorithm are consistently less than that of Becker-Li for the four seasons.

As mentioned by the Becker and Li (1995), the performance of LST retrieval algorithms depends primary on the quality of radiative transfer models, the characteristics of atmospheric profiles and surface from which the LST algorithms have been developed. The four LST retrieval algorithms used in this study have been developed to fit the NOAA/AVHRR channels 4 and 5, and the regions where the authors have concerns. And there are some differences in the band width and spectral response function between AVHRR channels 4 (10.3-11.30 μm) and 5 (11.50-12.50 μm) and MODIS channels 31 (10.78-11.28 μm) and 32 (11.77-12.27 μm). Also there should be some differences in the atmospheric environments and the surface conditions between the regions targeted by authors and the Korean Peninsula. So, when we take into account the above-mentioned facts, the results should be understood not in quantitative sense but in qualitative sense. The results suggest that it is necessary to develop LST algorithm for the retrieval of LST over Korean Peninsula using the atmospheric profiles and surface conditions of this region.

Acknowledgements

This research was supported by the "Development of Meteorological Data Processing System of Communication, Ocean and Meteorological Satellite (V)".

References

Becker, F. and Z.-L. Li, 1990. Toward a local split window method over land surface. *Int. J. Remote Sens.*, 3: 369-393.

Carlson, T. N., J. A. Augustine, and F. E. Boland, 1977. Potential application of satellite temperature measurements in the analysis of land use over urban areas. *Bull. Amer. Meteor. Soc.*, 58: 1301-1304.

Choi, H. S. and H. G. Cho, 1986. Estimation of surface temperature derived from GMS radiance observations over South Korea, *J. Korean Meteor. Soc.*, 22(1): 82-99.

Coll, C., Caselles, T. V., Galve, J. M., Valor, E., Niclo's, R., Sanchez, J. M., and Rivas, R., 2005. Ground measurements for the validation of land surface temperatures derived from AATSR and MODIS data Remote Sensing of Environment, 97: 288 - 300.

Gutman, G. and A. Ignatov, 1998. The derivation of the green vegetation fraction from NOAA/AVHRR data for use in numerical weather prediction models. *Int. J. Remote Sens.*, 19(8): 1533-1543.

Han, K. -S., A. A. Viau, and F. Anctil, 2004. An analysis of GOES and NOAA derived land surface temperatures estimated over a boreal forest. *Int. J. Remote Sens.*, 25(21): 4761-4780.

Kang, J.-H., M.-S. Suh, C.-H. Kwak, and Y.-S. Lee, 2005. 10. 27~28, Classification of land cover over Korean Peninsula using MODIS data, *Proceedings of Korean Meteorological Society*, 400-401pp.

Kerr, Y. H., J. P Lagouarde, and J. Imbernon, 1992. Accurate land surface temperature retrieval from AVHRR data with use of an improved split window, *Remote Sensing of Environment*, 41: 197-209.

Peres, L. F. and C. C. DaCamara, 2002. An emissivity look-up table for LST estimation from MSG data. *SAF Training Workshop Proceedings*. 48-55pp.

Prata, A. J. and R. P. Cechet, 1999. An assessment of the accuracy of land surface temperature determination from the GMS-5 VISSR. *Remote Sensing of Environment*, 67: 1-14.

Price, J. C., 1984. Land surface temperature measurements from the split window channels of the NOAA-7 Advanced Very High Resolution Radiometer. *Journal of Geophysical Research*, 89: 7231-7237.

Salisbury, J. W. and M. D'Aria, 1992. Emissivity of terrestrial materials in the 8-14 μm atmospheric window, *Remote Sensing of Environment*, 42: 83-106.

Saunders, R. W. and K. T. Kriebel, 1988. An improved method for detecting clear sky and cloudy radiances from AVHRR data. *Int. J. Remote Sens.*, 9: 123-150.

Shin, S.-H., K.-J Ha, J.-H. Kim, H.-M. Oh, and M.-H. Jo, 2004. Estimation of local surface temperature from EBM with the use of GRID/GIS and remote sensed data. *Korean Journal of Remote Sensing*, 20(2): 103-116

Sikorski, R. J. and P. S. Kealy, 2002. Land surface temperature - Visible/infrared imager/ radiometer suite algorithm theoretical basis document v5.0, Raytheon Systems Company, 35pp.

Sobrino, J. A. and N. Raissouni, 2000. Toward remote sensing methods for land cover dynamic monitoring: application to Morocco. *Int. J. Remote Sens.*, 21(2): 353-366.

Sobrino, J. A. and M. Romaguera, 2004. Land surface temperature retrieval from MSG1-SEVIRI data. *Remote Sensing of Environment*, 92: 247-254.

Suh, M.-S. and D.-K. Lee, 1999. Development of cloud detection algorithm for extracting the cloud-free land surface from day time NOAA/AVHRR data, *Korean Journal of Remote Sensing*, 15(3): 239-251.

Ulivieri, C., M. M. Castronouvo, R. Francioni, and A. Cardillo, 1994. A split-window algorithm for estimating land surface temperature from satellites. *Advances in Space Research*, 14(3): 59-65.

Valor, E. and V. Caselles, 1996. Mapping land surface emissivity from NDVI: Application to European, African, and South American areas, *Remote Sensing of Environment*, 57: 164-184.

Vázquez, D. Pozo. F. J. Olmo Reyes, and L. Alados Arboledas, 1997. A comparative study of algorithms for estimating land surface temperature from AVHRR data, *Remote Sensing of Environment*, 62: 216-222.

Wan, Z. and J. Dozier, 1996. A generalized split-window algorithm for retrieving of land surface temperature from space, *IEEE Trans. Geosci. Remote Sensing*, 34: 892-905.

Watson, K., 1992. Two-temperature method for measuring emissivity, *Remote sensing of Environment*, 42: 117-12.

Wan, Z., Zhanga, Y., Zhanga, Q., and Li, Z.-L., 2005. Validation of the land-surface temperature products retrieved from Terra Moderate Resolution Imaging Spectroradiometer data, *Remote Sensing of Environment*, 83: 163-180.